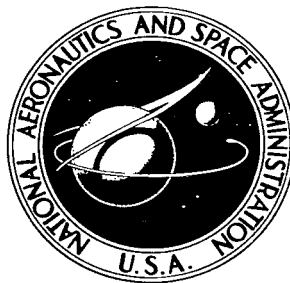


NASA TECHNICAL NOTE



NASA TN D-4260

2.1

NASA TN D-4260

LOAN COPY: RE
AFWL (WL
KIRTLAND AFB

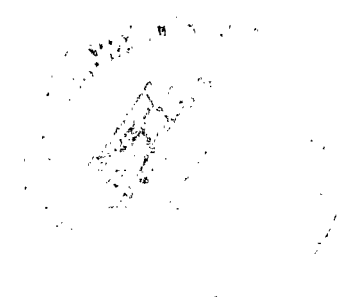
0130972



TECH LIBRARY KAFB, NM

THREE BALLISTIC CAMERA DATA REDUCTION METHODS APPLICABLE TO REENTRY EXPERIMENTS

by John E. Hogge
Langley Research Center
Langley Station, Hampton, Va.





THREE BALLISTIC CAMERA DATA REDUCTION METHODS
APPLICABLE TO REENTRY EXPERIMENTS

By John E. Hogge

Langley Research Center
Langley Station, Hampton, Va.

NATIONAL AERONAUTICS AND SPACE ADMINISTRATION

For sale by the Clearinghouse for Federal Scientific and Technical Information
Springfield, Virginia 22151 - CFSTI price \$3.00

THREE BALLISTIC CAMERA DATA REDUCTION METHODS APPLICABLE TO REENTRY EXPERIMENTS

By John E. Hogge
Langley Research Center

SUMMARY

Ballistic cameras were used by the Langley Research Center to photograph a reentry test object against a star background in order to determine accurately the position, velocity, and deceleration of the object as it penetrates the earth's atmosphere. Three data reduction methods which are applicable to the determination of the reentry trajectories from the photographic records are discussed. One reduction method applies when the reentry image on each photographic plate can be approximated with a straight line. Another method applies when the reentry image is curved on each photographic plate. A third technique applies when the shutter of each of several cameras at different stations is synchronized in time.

INTRODUCTION

Reentry experiments employing multistage rockets were performed from the NASA Wallops Station launch site at Wallops Island, Va., to investigate the physical phenomena which occur during reentry of high-speed objects into the earth's atmosphere. The first several stages lifted a velocity package (the reentry stages) up to a predetermined altitude; then the remaining stages were sequentially fired downward so that the last stage after burnout served as the reentry test object. Ionization and dissociation of body material and atmospheric gases produced a visible reentry trace against a star background. Ballistic camera exposures of the reentry trace against a star background were used to determine the position, velocity, and deceleration of the reentry object as it penetrates the atmosphere.

A number of ballistic cameras were employed at the three NASA camera stations at Coquina Beach, N.C., Wallops Island, and Sandbridge, Va. At least one ballistic camera at each site was equipped with a time-controlled shutter to provide a programmed sequence of exposures of the reentry trace for velocity determination. A camera network, consisting of one ballistic camera at each site, were synchronized in time — that is, each of the shutters opened and closed at the same instant of time. If all three cameras were successful in acquiring the reentry trace, then photogrammetric triangulation for the

position of the reentry object as a function of time could be performed. When the reentry photographs were available only from nonsynchronized cameras, then other reduction techniques could be used.

The purpose of this report is to summarize the methods and procedures that are available at the Langley Research Center for reducing raw photographic reentry data to final trajectory parameters. This reduction capability was established primarily for the Trailblazer I and II series of reentry experiments which are described in references 1 and 2.

Each of the data reduction methods discussed herein is written in the FORTRAN (FORMula TRANslation) II language for the IBM 7094 electronic data processing system.

SYMBOLS

λ^1, μ^1, ν^1	direction cosines referred to equinox 1
λ^2, μ^2, ν^2	direction cosines referred to equinox 2
α_s, δ_s	right ascension and declination of a star
x_s, y_s	star image plate coordinates measured relative to an orthogonal system (x,y) on plate
A,B	camera or station
A_p, B_p	photographic plates from cameras A and B, respectively
b,e	reentry image points on B_p
$\vec{K}_{Bb}, \vec{K}_{Be}$	unit vectors defining rays through projection center of camera B and end points b and e on B_p
B_b	reentry point corresponding to image point b on B_p
B_e	reentry point corresponding to image point e on B_p
$BB_b B_e$	plane defined by camera B and the reentry
$\lambda_{Bb}, \mu_{Bb}, \nu_{Bb}$	direction cosines of \vec{K}_{Bb}

$\lambda_{Be}, \mu_{Be}, \nu_{Be}$	direction cosines of \vec{K}_{Be}
$\vec{i}, \vec{j}, \vec{k}$	unit vector along X-, Y-, and Z-axis, respectively
L_B	arc length of the reentry as seen from camera B, radians
$\lambda_{BP}, \mu_{BP}, \nu_{BP}$	direction cosines of a normal to plane BB_bB_e defined by camera B and the reentry
S_A	perpendicular distance from station A to plane BB_bB_e
\vec{P}_{BP}	unit vector along the normal to plane BB_bB_e
X_{AB}, Y_{AB}, Z_{AB}	relative rectangular coordinates of station B with respect to station A
R_{AB}	distance between stations A and B
m	reentry image point on A_p corresponding to beginning of a shutter break in data reduction method I
M	reentry point corresponding to image point m
\vec{K}_{Am}	unit vector defining a ray through station A and points m and M
R_{Am}	slant range from station A to reentry point M
ω_m	angle between \vec{S}_A and \vec{R}_{Am} (see fig. 4)
W	intersection of \vec{S}_A with plane BB_bB_e
$\lambda_{Am}, \mu_{Am}, \nu_{Am}$	direction cosines of \vec{K}_{Am}
X_{Am}, Y_{Am}, Z_{Am}	rectangular coordinates of reentry point M with respect to X, Y, Z centered at station A
d_m	spatial length corresponding to mth shutter break on reentry image on A_p

X, Y, Z	astronomical equatorial coordinate system centered at station A
ϕ_i'	geocentric latitude of ith camera station
ϕ_i	geodetic latitude of ith camera station
a	semimajor axis of reference ellipsoid for earth, 6378.388 km
R_i	radial distance to ith camera station from center of earth
δR_i	altitude of ith camera station above mean sea level
θ_i	sidereal time at ith station corresponding to instant of reentry
θ_0	sidereal time at Greenwich for zero hours universal time on night of reentry
UT	universal time of reentry
Λ_i	west longitude of ith camera station
ξ_0, η_0	standard coordinates of an object
$\lambda_\xi, \mu_\xi, \nu_\xi$	direction cosines of ξ -axis
$\lambda_\eta, \mu_\eta, \nu_\eta$	direction cosines of η -axis
λ_0, μ_0, ν_0	direction cosines of an object ray
λ_c, μ_c, ν_c	direction cosines of central ray
α_c, δ_c	right ascension and declination of central ray
α_0, δ_0	right ascension and declination of an object
x_0, y_0	measured plate coordinates of an object
ξ_s, η_s	standard coordinates of star image

$\Delta x, \Delta y$	difference between measured and computed values of star image plate coordinates
x, y	orthogonal coordinate system in plane of photograph; all points of interest on plate are measured with respect to this system
x_i, y_i	plate measurements on reentry image
U	line connecting center of projection of camera A with some arbitrary point on the reentry
Q	line connecting center of projection of camera B with a particular point on the reentry
λ_i, μ_i, ν_i	direction cosines of U
λ_j, μ_j, ν_j	direction cosines of Q
X_u, Y_u, Z_u	coordinates of an arbitrary point u on line U
X_q, Y_q, Z_q	coordinates of an arbitrary point q on line Q
D	distance between point u on line U and point q on line Q
X_{Aj}, Y_{Aj}, Z_{Aj}	Cartesian coordinates of reentry point relative to station A and corresponding to jth image measurement on chopped plate B
X', Y', Z'	camera axis system in data reduction method III
$\bar{X}_A, \bar{Y}_A, \bar{Z}_A$	location of camera A with respect to fixed reference system $\bar{X}, \bar{Y}, \bar{Z}$ in data reduction method III
c	focal length of camera
x_p, y_p	coordinates of plate center in data reduction method III, measured relative to x,y system

$\left. \begin{array}{l} \lambda_1, \mu_1, \nu_1 \\ \lambda_2, \mu_2, \nu_2 \\ \lambda_3, \mu_3, \nu_3 \end{array} \right\}$	direction cosines relating camera-fixed axes and space-fixed axes in data reduction method III
X_0, Y_0, Z_0	initial approximation to reentry point
ϵ_x, ϵ_y	error equations in least-squares process of data reduction method III
$\sigma_1, \sigma_2, \sigma_3$	angles relating camera-fixed axes to space-fixed axes in data reduction method III
d	spatial distance along reentry trajectory
t	time
V	velocity
\dot{V}	deceleration
Superscripts:	
h	hours of time
s	seconds of time

IDENTIFICATION OF STELLAR AND REENTRY EXPOSURES

A sketch of a reentry, photographed against a star background, is shown in figure 1. This sketch represents a photograph which was taken with a stationary camera equipped with a time-controlled shutter – that is, a shutter programed to open and close at specified time intervals. Hence, both the reentry and stellar images consist of trails which are broken into time-dependent segments. Programed exposures of the star field are made before and after reentry, with the post-reentry exposures made in the reverse time sequence. As can be observed from the figure, breaks in the star trails during the reentry period are not resolved; this is due to the rapid shutter rate which was programed for the reentry mode. The time associated with each break on the star trails is determined from the initial time of camera opening and the subsequent shutter rate. The time corresponding to the occurrence of reentry is recorded at the camera site. Figure 2 is a

sketch of a typical photographic plate from a streaked camera – that is, from a camera that is not equipped with a time-controlled shutter. Note that both the reentry and star images are continuously trailed on the plate.

From each photographic plate utilized in the reduction to final trajectory parameters, a number of selected reference stars are chosen in the vicinity of the reentry images for the purpose of determining constants of the camera system. These constants appear in the transformation from photographic plate coordinates to standard coordinates relative to a perfect projection plane in data reduction methods I and II and are subsequently used to correct for errors and camera system distortions in the data reduction. The reference stars are utilized in data reduction method III in the determination of camera orientation and other physical parameters of the camera system. The right ascension and declination of each reference star relative to the equinox of the beginning of the year nearest to the time of exposure are needed in the reduction methods. These quantities are determined in the following manner. The overall star field on the photographic plate is identified with the aid of appropriate star charts. By visually comparing the plate with the star chart, approximate values of the celestial coordinates are read from the gridded star chart. With these approximations, the stars are identified in the Boss star catalog and the right ascension and declination relative to the epoch of the catalog (1950.0) are established. After these coordinates are corrected for proper motion, they are written in terms of direction cosines and transformed from the catalog epoch to the beginning of the year nearest to the time of exposure. According to reference 3, this transformation becomes

$$\begin{bmatrix} \lambda^2 \\ \mu^2 \\ \nu^2 \end{bmatrix} = \begin{bmatrix} X_x & X_y & X_z \\ Y_x & Y_y & Y_z \\ Z_x & Z_y & Z_z \end{bmatrix} \begin{bmatrix} \lambda^1 \\ \mu^1 \\ \nu^1 \end{bmatrix}$$

where λ^1, μ^1, ν^1 and λ^2, μ^2, ν^2 are the direction cosines of the star relative to the epoch of the catalog and the year nearest to exposure time, respectively. In terms of the right ascension α_s and declination δ_s of the star,

$$\lambda^1 = \cos \delta_s \cos \alpha_s$$

$$\mu^1 = \cos \delta_s \sin \alpha_s$$

$$\nu^1 = \sin \delta_s$$

The elements of the transformation matrix are defined and tabulated for the beginning of each year from 1900-1980 in reference 4, page 109.

In addition to the celestial coordinates (right ascension and declination) of each reference star, the relative rectangular coordinates x, y of reference star images and points along the reentry traces, measured in the plane of the photographic plate, are required. On chopped plates, the beginning and end of each shutter break on the reentry trace are measured. Some convenient break in the star trails is measured with time corresponding to that particular break noted. On streaked plates, the beginning or end of the star exposure is measured. The procedure for measuring streaked reentry images varies with the technique of reduction and is therefore discussed with each reduction method.

Precision comparators are employed at the Langley Research Center to perform photographic plate measurements. These machines have the capability of measuring relative distance of points on the plate to within ± 5 microns over the entire travel of the engine ways.

DATA REDUCTION METHOD USING STRAIGHT-LINE REENTRY IMAGES

The method which uses a straight-line approximation to the reentry image on each plate (herein referred to as data reduction method I) is essentially the method discussed in reference 3. This analysis technique was developed for the reduction of meteor trails observed simultaneously from two camera sites. In the solution for the spatial position of each shutter break, the assumption is made that the reentry is part of a great circle when projected onto the celestial sphere. If this assumption is valid, the reduction of photographic plate coordinates to final position, velocity, and deceleration can be performed with nonsynchronized pairs of photographs. Furthermore, a complete reduction can be made when only one of the photographic images is chopped. These features have led to extensive use of this analysis technique for the reduction of trajectory parameters from photographic observations. A general description of the method as it was applied to the reentry problem is given herein. Much of the details of the technique is omitted since a complete discussion can be found in reference 3. However, a derivation of some of the working equations is given in the appendixes herein to present the geometrical connection of the camera network parameters to these equations.

To illustrate the technique, it is assumed that one of the photographic plates is not chopped and is arbitrarily chosen to be plate B in figure 3. Furthermore, it is assumed that the reentry image forms a straight segment on plate B and that reentry image breaks on plate A can be connected with a straight line. In figure 4, A and B denote the cameras from which the plates A_p and B_p were obtained.

To establish the plane BB_bB_e through the center of projection of camera B and the reentry, two points on the reentry image are selected. One point should be near the beginning of the reentry image and the other point should be near the end as indicated by b and e, respectively, in figure 3. Unit vectors \vec{K}_{Bb} and \vec{K}_{Be} (fig. 4) define rays through the projection center and the end points b and e on the photographic plate. These rays pass through the reentry points B_b and B_e . The unit vectors can be written

$$\vec{K}_{Bb} = \vec{i}\lambda_{Bb} + \vec{j}\mu_{Bb} + \vec{k}\nu_{Bb}$$

and

$$\vec{K}_{Be} = \vec{i}\lambda_{Be} + \vec{j}\mu_{Be} + \vec{k}\nu_{Be}$$

where \vec{i} , \vec{j} , and \vec{k} are unit vectors along the X, Y, and Z axes and $\lambda_{Bb}, \mu_{Bb}, \nu_{Bb}$ and $\lambda_{Be}, \mu_{Be}, \nu_{Be}$ are the direction cosines of \vec{K}_{Bb} and \vec{K}_{Be} , respectively. These direction cosines are relative to the reference coordinate system which at this point is defined only to be centered at camera A.

Direction cosines of a normal to the plane BB_bB_e , defined by station B and the reentry points B_b and B_e , are determined from \vec{K}_{Bb} and \vec{K}_{Be} to be

$$\left. \begin{aligned} \lambda_{BP} &= \frac{\mu_{Bb}\nu_{Be} - \nu_{Bb}\mu_{Be}}{\sin L_B} \\ \mu_{BP} &= \frac{\nu_{Bb}\lambda_{Be} - \lambda_{Bb}\nu_{Be}}{\sin L_B} \\ \nu_{BP} &= \frac{\lambda_{Bb}\mu_{Be} - \mu_{Bb}\lambda_{Be}}{\sin L_B} \end{aligned} \right\} \quad (1)$$

where L_B is the arc length of the reentry in radians, as seen from station B, and is determined from observing that

$$\lambda_{BP}^2 + \mu_{BP}^2 + \nu_{BP}^2 = 1$$

The perpendicular distance S_A from camera A to the plane BB_bB_e is given by

$$S_A = \vec{P}_{BP} \cdot \vec{R}_{AB} = X_{AB}\lambda_{BP} + Y_{AB}\mu_{BP} + Z_{AB}\nu_{BP}$$

where

$$\vec{P}_{BP} = \vec{i}\lambda_{BP} + \vec{j}\mu_{BP} + \vec{k}\nu_{BP}$$

$$\vec{R}_{AB} = \vec{i}X_{AB} + \vec{j}Y_{AB} + \vec{k}Z_{AB}$$

and X_{AB}, Y_{AB}, Z_{AB} are the relative rectangular coordinates of camera B with respect to camera A.

The unit vector \vec{K}_{Am} (fig. 4) defines a ray through the center of projection of camera A and some measured shutter break m on A_p . In terms of direction cosines,

$$\vec{K}_{Am} = \vec{i}\lambda_{Am} + \vec{j}\mu_{Am} + \vec{k}\nu_{Am}$$

The intersection of this ray with the plane BB_bB_e is the point on the reentry M whose image on A_p is m . The coordinates of this point X_{Am}, Y_{Am}, Z_{Am} are determined as follows.

The slant range R_{Am} from station A to point M is determined from the right triangle AWM in figure 4 by the equation

$$R_{Am} = S_A \sec \omega_m \quad (2)$$

where W is the intersection of \vec{S}_A with the plane BB_bB_e and ω_m is the angle between \vec{S}_A and \vec{R}_{Am} . From figure 4,

$$\vec{P}_{BP} \cdot \vec{K}_{Am} = \cos \omega_m = \lambda_{BP}\lambda_{Am} + \mu_{BP}\mu_{Am} + \nu_{BP}\nu_{Am}$$

and hence

$$R_{Am} = \frac{X_{AB}\lambda_{BP} + Y_{AB}\mu_{BP} + Z_{AB}\nu_{BP}}{\lambda_{BP}\lambda_{Am} + \mu_{BP}\mu_{Am} + \nu_{BP}\nu_{Am}} \quad (3)$$

The components of \vec{R}_{Am} along the reference axis are

$$\left. \begin{aligned} X_{Am} &= R_{Am} \lambda_{Am} \\ Y_{Am} &= R_{Am} \mu_{Am} \\ Z_{Am} &= R_{Am} \nu_{Am} \end{aligned} \right\} \quad (4)$$

The application of equation (4) to the beginning and end of each shutter break on the photographic plate results in the X,Y,Z coordinates of the corresponding points in space relative to camera A. The spatial length corresponding to a particular shutter break on the plate is

$$d_m = \left[(X_{Am+1} - X_{Am})^2 + (Y_{Am+1} - Y_{Am})^2 + (Z_{Am+1} - Z_{Am})^2 \right]^{1/2} \quad (5)$$

where subscripts m and m+1 denote the beginning and the end of a break, respectively.

In order to apply equations (1) to (5), direction cosines of points along the reentry trajectory as seen from both camera sites and the relative coordinates of station B with respect to station A must be determined. The direction cosines are determined from measurements on the photographic plates and the relative station coordinates are found from a knowledge of the station location (longitude, latitude, and altitude above sea level) and the time at which the reentry occurred. A discussion of each of these computations follows.

The axis system shown in figure 4 is an astronomical equatorial system centered at station A. The X-axis points toward the equinox of date and the Y-axis lies 90° east in the plane parallel to the equator. The Z-axis is chosen to form a right-hand coordinate system. Hence, the coordinates of station B with respect to station A are functions of time. To calculate these coordinates, certain auxiliary computations are necessary. These computations include the earth's local radius at each camera site, conversion of geodetic latitude to geocentric latitude, and the sidereal time at each camera station corresponding to the time of reentry.

For the reduction of reentry photographic observations, the International Ellipsoid is used to represent the mean sea level of the earth. Based on this reference model, the geocentric latitude of and the radial distance from the center of the earth to the ith camera station are determined from the following equations from reference 5 (p. 489):

$$\phi_i' = \phi_i - 11' 35''.6635 \sin 2\phi_i + 1''.1731 \sin 4\phi_i - 0''.0026 \sin 6\phi_i \quad (6)$$

and

$$R_i = a \left(0.998320047 + 0.1683494 \times 10^{-2} \cos 2\phi_i - 0.3549 \times 10^{-5} \cos 4\phi_i + 0.8 \times 10^{-8} \cos 6\phi_i \right) + \delta R_i \quad (7)$$

where

ϕ_i geodetic latitude of ith camera

ϕ_i' geocentric latitude of ith camera

a semimajor axis of reference ellipsoid, 6378.388 km

R_i radial distance from earth's center to ith camera station

δR_i altitude of ith camera station above mean sea level

The sidereal time at the ith station θ_i corresponding to the instant of reentry is computed from

$$\theta_i = \theta_0 + (UT) - \Lambda_i + \Delta\theta^S$$

where

θ_0 sidereal time at Greenwich for 0^h universal time on night of reentry

UT universal time of reentry

Λ_i west longitude of ith station

$$\Delta\theta^S = 236.555(UT^h/24^h)$$

s, h seconds and hours of time, respectively

With these parameters determined, the relative rectangular coordinates of station B with respect to station A at the instant of reentry are computed from the following equations which are developed in appendix A:

$$\left. \begin{aligned}
X_{AB} &= [R_B \cos \phi_B' \cos(\Lambda_B - \Lambda_A) - R_A \cos \phi_A'] \cos \theta_A - [R_B \cos \phi_B' \sin(\Lambda_B - \Lambda_A)] \sin \theta_A \\
Y_{AB} &= [R_B \cos \phi_B' \sin(\Lambda_B - \Lambda_A)] \cos \theta_A + [R_B \cos \phi_B' \cos(\Lambda_B - \Lambda_A) - R_A \cos \phi_A'] \sin \theta_A \\
Z_{AB} &= R_B \sin \phi_B' - R_A \sin \phi_A'
\end{aligned} \right\} (8)$$

The distance between the two camera stations is given by

$$R_{AB} = (X_{AB}^2 + Y_{AB}^2 + Z_{AB}^2)^{1/2}$$

To calculate the direction cosines of points along the reentry trajectory, by utilizing the measured plate coordinates, the method of standard coordinates (see appendix B) is used. This method assumes that the photographic plate is a perfect projection of the object space; that is, points on the celestial sphere are projected through its center (projection center of the camera) onto a plane surface (the photographic plate).

If the right ascension and declination of the central projection ray (i.e., the ray normal to the projection plane) and an object in space are known, the standard coordinates of the object (appendix B) are given by

$$\left. \begin{aligned}
\xi_o &= \frac{\lambda_o \lambda_\xi + \mu_o \mu_\xi}{\lambda_o \lambda_c + \mu_o \mu_c + \nu_o \nu_c} \\
\eta_o &= \frac{\lambda_o \lambda_\eta + \mu_o \mu_\eta + \nu_o \nu_\eta}{\lambda_o \lambda_c + \mu_o \mu_c + \nu_o \nu_c}
\end{aligned} \right\} (9)$$

where

$$\begin{aligned}
\lambda_o &= \cos \delta_o \cos \alpha_o & \lambda_c &= \cos \delta_c \cos \alpha_c \\
\mu_o &= \cos \delta_o \sin \alpha_o & \mu_c &= \cos \delta_c \sin \alpha_c \\
\nu_o &= \sin \delta_o & \nu_c &= \sin \delta_c \\
\lambda_\eta &= -\sin \delta_c \cos \alpha_c & \lambda_\xi &= -\sin \alpha_c \\
\mu_\eta &= -\sin \delta_c \sin \alpha_c & \mu_\xi &= \cos \delta_c \\
\nu_\eta &= \cos \delta_c & \nu_\xi &= 0
\end{aligned}$$

and α_c, δ_c and α_o, δ_o denote the right ascension and declination of the central ray and the object, respectively.

The ξ and η coordinates are relative to the perfect projection plane. If the central ray is taken to be the plane center, then for each object whose right ascension and declination are known the corresponding standard coordinates can be computed from equations (9). Conversely, if the standard coordinates of an object are known, the direction of the object in space can be determined by the inverse relationships

$$\left. \begin{aligned} \lambda_o &= \frac{\lambda_c + \lambda_\eta \eta_o + \lambda_\xi \xi_o}{\sqrt{1 + \xi_o^2 + \eta_o^2}} \\ \mu_o &= \frac{\mu_c + \mu_\eta \eta_o + \mu_\xi \xi_o}{\sqrt{1 + \xi_o^2 + \eta_o^2}} \\ \nu_o &= \frac{\nu_c + \nu_\eta \eta_o}{\sqrt{1 + \xi_o^2 + \eta_o^2}} \end{aligned} \right\} \quad (10)$$

where λ_o , μ_o , and ν_o denote the direction cosines of the object with respect to an astronomical equatorial coordinate system centered at camera A. Hence, the direction of points along the reentry trajectory is determined once the corresponding standard coordinates are computed.

It is assumed that the measured plate coordinates of an object x_o, y_o are linearly related to the standard coordinates ξ_o, η_o by

$$\left. \begin{aligned} x_o &= a_x \xi_o + b_x \eta_o + c_x \\ y_o &= a_y \xi_o + b_y \eta_o + c_y \end{aligned} \right\} \quad (11)$$

where $a_x, b_x, c_x, a_y, b_y,$ and c_y are plate constants to be determined. Approximately 10 reference stars, whose right ascension and declination are known, are selected in the vicinity of the reentry image on the photographic plate. The star coordinates are measured as described in reference 3. Therefore, both the measured coordinates x_s, y_s and the standard coordinates ξ_s, η_s are available since the right ascension and declination for each reference star is known. With this information, the plate constants appearing in equations (11) are determined by the method of least squares. Once these plate constants are established, the inverse relationships are used to determine the standard coordinates and, hence, the direction cosines of any point of interest on the photographic plate from the comparator measurements. Therefore, the standard

coordinates of points along the reentry trajectory are determined from the photographic image measurements x_0, y_0 and the inverse of equations (11)

$$\left. \begin{aligned} \xi_0 &= a_\xi x_0 + b_\xi y_0 + c_\xi \\ \eta_0 &= a_\eta x_0 + b_\eta y_0 + c_\eta \end{aligned} \right\} \quad (12)$$

where

$$\begin{aligned} a_\xi &= \frac{b_y}{c_{xy}} & b_\xi &= \frac{-b_x}{c_{xy}} & c_\xi &= \frac{-b_y c_x + b_x c_y}{c_{xy}} \\ a_\eta &= \frac{-a_y}{c_{xy}} & b_\eta &= \frac{a_x}{c_{xy}} & c_\eta &= \frac{a_y c_x - a_x c_y}{c_{xy}} \end{aligned}$$

and

$$c_{xy} = a_x b_y - a_y b_x$$

Before the standard coordinates of reentry points are computed, the measurements on the reentry image are corrected as described in reference 3 for optical and emulsion distortions as well as for incorrect identification of the plate center, differential aberration, differential refraction, and errors in the comparators. These corrections are performed as follows:

With the plate constants determined, standard coordinates of reference stars are substituted into equations (11) and the corresponding plate coordinates are computed. The computed coordinates are compared with the measured coordinates and the differences Δx and Δy are used to correct the plate measurements of the reentry image. For the ballistic cameras employed in the optical coverage, the plate residuals Δx and Δy were on the order of a few microns. The plate residuals Δx and Δy are plotted separately against x along the reentry image and the points are connected with smooth curves. Corrections are read from these graphs and applied to the reentry image measurements. The standard coordinates are then determined from the corrected measurements through the application of equations (11), and then the direction cosines of the reentry points are computed from equations (10).

DATA REDUCTION METHOD USING CURVED REENTRY IMAGES

Data reduction method I has the advantage that, if the reentry images on the plate can be approximated with a straight line, a complete reduction is possible when one chopped plate is used in conjunction with a streaked plate from a different camera site. Also, a complete reduction can be made when two nonsynchronized chopped plates are used. A modification to data reduction method I, applicable to the reduction of non-synchronized pairs of photographs where the reentry images show definite curvature, was made. A description of this technique (data reduction method II) with some of the working equations developed in appendix C follows.

Sketches of a streaked photograph and a chopped photograph of a curved reentry are shown in figure 5. On the chopped plate, measurements of the beginning and end of each shutter break are made as data reduction method I. Reentry image measurements on the streaked plate are made at 250-micron intervals along the image. If the curvature of the image is smooth, a third-order polynomial is fitted through the measurements by the method of least squares; hence, for any x_i along the image

$$y_i = \beta_0 + \beta_1 x_i + \beta_2 x_i^2 + \beta_3 x_i^3 \quad (13)$$

where the constants $\beta_0, \beta_1, \beta_2, \beta_3$ which appear in equation (13) are determined from the least-squares fit.

As described in data reduction method I, if the corrected plate coordinates x_i and y_i are given, the corresponding direction cosines can be determined. By evaluating equation (13), at a few micron increments in the x-direction, a set of direction cosines corresponding to each increment can be tabulated.

In figure 6, A denotes the camera corresponding to the streaked photograph. Let the line U emanating from camera A be defined by direction cosines λ_i, μ_i, ν_i obtained from some arbitrary point x_i, y_i on the curved streak on plate A. The line Q beginning at camera B and extending in space has direction cosines λ_j, μ_j, ν_j , which are determined from some measured shutter break x_j, y_j on the chopped plate.

The distance between lines U and Q is

$$D = \sqrt{(X_u - X_q)^2 + \left[\frac{\mu_i}{\lambda_i} X_u - \frac{\mu_j}{\lambda_j} (X_q - X_{AB}) - Y_{AB} \right]^2 + \left[\frac{\nu_i}{\lambda_i} X_u - \frac{\nu_j}{\lambda_j} (X_q - X_{AB}) - Z_{AB} \right]^2} \quad (14)$$

As derived in appendix C, equation (14) yields the minimum value of D when

$$X_u = \frac{\lambda_i(B_i - C_j A_{ij})}{1 - A_{ij}^2}$$

$$X_q = \frac{\lambda_j(B_i A_{ij} - C_j)}{1 - A_{ij}^2} + X_{AB}$$

where

$$B_i = \lambda_i X_{AB} + \mu_i Y_{AB} + \nu_i Z_{AB}$$

$$C_j = \lambda_j X_{AB} + \mu_j Y_{AB} + \nu_j Z_{AB}$$

$$A_{ij} = \lambda_i \lambda_j + \mu_i \mu_j + \nu_i \nu_j$$

X_{AB}, Y_{AB}, Z_{AB} are the relative station coordinates, and the subscripts i and j refer to plates A and B , respectively.

Among all the sets of direction cosines λ_i, μ_i, ν_i computed by evaluating the polynomial fit to the curved streaked reentry, one set gives D a relative minimum value. This relative minimum value is determined by evaluating D for every set of direction cosines and choosing the smallest value. It is assumed that the set λ_i, μ_i, ν_i which gives rise to the relative minimum distance D defines a line which passes through the point on the reentry trajectory corresponding to the measured shutter break on the chopped plate. Hence, a triangulation is performed with the two rays and the vector \vec{R}_{AB} , which is shown in figure 6 and described in data reduction method I. This operation results in the spatial coordinates, relative to camera A , of the reentry point corresponding to the shutter break. The rectangular coordinates of the reentry point are given by

$$\left. \begin{aligned} X_{Aj} &= \frac{\lambda_i(B_i - C_j A_{ij})}{1 - A_{ij}^2} \\ Y_{Aj} &= \frac{\mu_i}{\lambda_i} X_{Aj} \\ Z_{Aj} &= \frac{\nu_i}{\lambda_i} X_{Aj} \end{aligned} \right\} \quad (15)$$

and the slant range becomes

$$R_{Aj} = \frac{B_i - C_j A_{ij}}{1 - A_{ij}^2}$$

These expressions for the spatial coordinates are evaluated by using the set of direction cosines λ_i, μ_i, ν_i that gave D a relative minimum value. By the application of this analysis technique to the beginning and the end of each shutter break on the chopped plate, the spatial components of each of these points on the reentry trajectory can be determined and, hence, the distance between points can be computed.

DATA REDUCTION METHOD USING SYNCHRONOUS PHOTOGRAPHS

For synchronized photographs, the data reduction method (herein referred to as data reduction method III) described in reference 6 is applicable. Since the details of the theory are developed therein, only a brief discussion of this technique with the working equations is given in this report. The notation for the working equations of reference 6 presented herein is that of the present report.

Figure 7 illustrates the connection between the image space (photograph) and the object space (reentry). The measured image coordinates x, y are related to the spatial coordinates X, Y, Z of the corresponding point on the reentry by

$$\left. \begin{aligned} x - x_p &= c \left[\frac{\lambda_1(X - \bar{X}_A) + \mu_1(Y - \bar{Y}_A) + \nu_1(Z - \bar{Z}_A)}{\lambda_3(X - \bar{X}_A) + \mu_3(Y - \bar{Y}_A) + \nu_3(Z - \bar{Z}_A)} \right] \\ y - y_p &= c \left[\frac{\lambda_2(X - \bar{X}_A) + \mu_2(Y - \bar{Y}_A) + \nu_2(Z - \bar{Z}_A)}{\lambda_3(X - \bar{X}_A) + \mu_3(Y - \bar{Y}_A) + \nu_3(Z - \bar{Z}_A)} \right] \end{aligned} \right\} \quad (16)$$

Two such equations, result from each camera in the network. The direction cosines $\lambda_1, \mu_1, \dots, \nu_3$ relate the camera-fixed axes X', Y', Z' to the fixed reference frame $\bar{X}, \bar{Y}, \bar{Z}$ which in this data reduction method is a local vertical system with origin at some desired latitude and longitude. The \bar{X} -axis points north, the \bar{Y} -axis lies 90° east in the tangent plane, and the \bar{Z} -axis lies along the local vertical. These direction cosines are functions of three angles σ_1, σ_2 , and σ_3 which are the azimuth, elevation, and roll of the camera, respectively. These camera orientation parameters are referred to in reference 6 as rotational elements of exterior orientation. The interior camera elements

x_p, y_p and c are the coordinates of the photographic plate center and the focal length of the camera, respectively. The plate center coordinates x_p, y_p are measured with respect to an axis system on the photographic plate. These six camera orientation constants are determined from a distribution of reference stars on the photographic plate. The technique for determining these constants by utilizing the reference stars is discussed subsequently. From a knowledge of the latitude, longitude, and altitude above mean sea level of station A, $\bar{X}_A, \bar{Y}_A, \bar{Z}_A$ with respect to the reference frame can be determined.

Equations (16) provide two conditions on three unknowns – the X, Y, Z coordinates of the reentry point corresponding to the measured coordinates x, y . If the orientation constants and the position of each camera in the network are known, then three cameras in the network will provide six conditions on the coordinates of the reentry point. Hence, an overdetermination of the solution for these coordinates is possible. The method of differential correction (ref. 7, pp. 309-311), utilizing the least-squares scheme, is employed to solve these equations. To apply this technique, the equations are linearized by keeping only first-order terms in a Taylor's series expansion of equations (16) about an initial approximation to the coordinates of the reentry point. The error equations whose squares are minimized in the least-squares solution are

$$\left. \begin{aligned} \epsilon_x &= f(X_0, Y_0, Z_0) + \left. \frac{\partial f}{\partial X} \right|_0 \Delta X + \left. \frac{\partial f}{\partial Y} \right|_0 \Delta Y + \left. \frac{\partial f}{\partial Z} \right|_0 \Delta Z - x + x_p \\ \epsilon_y &= g(X_0, Y_0, Z_0) + \left. \frac{\partial g}{\partial X} \right|_0 \Delta X + \left. \frac{\partial g}{\partial Y} \right|_0 \Delta Y + \left. \frac{\partial g}{\partial Z} \right|_0 \Delta Z - y + y_p \end{aligned} \right\} \quad (17)$$

where

$$f = c \left[\frac{\lambda_1 (X - \bar{X}_A) + \mu_1 (Y - \bar{Y}_A) + \nu_1 (Z - \bar{Z}_A)}{\lambda_3 (X - \bar{X}_A) + \mu_3 (Y - \bar{Y}_A) + \nu_3 (Z - \bar{Z}_A)} \right]$$

$$g = c \left[\frac{\lambda_2 (X - \bar{X}_A) + \mu_2 (Y - \bar{Y}_A) + \nu_2 (Z - \bar{Z}_A)}{\lambda_3 (X - \bar{X}_A) + \mu_3 (Y - \bar{Y}_A) + \nu_3 (Z - \bar{Z}_A)} \right]$$

$$\Delta X = X - X_0$$

$$\Delta Y = Y - Y_0$$

$$\Delta Z = Z - Z_0$$

X_0, Y_0, Z_0 is the initial approximation to the reentry point, and the o subscript to the partial derivatives imply that the partials are evaluated by using the initial approximation X_0, Y_0, Z_0 .

For one object point, two error equations ϵ_x and ϵ_y exist for each camera. The most probable position of the corresponding reentry point is the one for which the sum of the square of the errors (ϵ 's) is minimized.

Through the least-squares process ΔX , ΔY , and ΔZ are determined from the initial approximation. These quantities are added to the initial approximation to give a new approximation to X, Y, Z . Substitution of this new approximation into equations (16) shows the extent to which these equations are satisfied. If equations (16) are not satisfied within some prescribed limit, the computed values of X , Y , and Z are used as a new approximation and the process is repeated until convergence is obtained. The values for the variables which result in convergence are the most probable position coordinates of the reentry point. This technique is applied to the beginning and end of each shutter break on the photographic plate. Hence, the spatial coordinates of points along the reentry trajectory corresponding to each shutter break are determined. The spatial distance corresponding to each shutter break on the plate can now be computed.

Equations (16) can be written in directional form by dividing both numerator and denominator of each equation by the magnitude of the slant range vector from the center of projection to the reentry point. The following equations result:

$$\left. \begin{aligned} x - x_p &= c \left(\frac{\lambda_1 \lambda + \mu_1 \mu + \nu_1 \nu}{\lambda_3 \lambda + \mu_3 \mu + \nu_3 \nu} \right) \\ y - y_p &= c \left(\frac{\lambda_2 \lambda + \mu_2 \mu + \nu_2 \nu}{\lambda_3 \lambda + \mu_3 \mu + \nu_3 \nu} \right) \end{aligned} \right\} \quad (18)$$

where λ , μ , and ν are the direction cosines of the object relative to the fixed-axis system and are expressed, respectively, as

$$\begin{aligned} \lambda &= \frac{X - \bar{X}_A}{R_A} \\ \mu &= \frac{Y - \bar{Y}_A}{R_A} \\ \nu &= \frac{Z - \bar{Z}_A}{R_A} \end{aligned}$$

with

$$\bar{R}_A = \left[(X - \bar{X}_A)^2 + (Y - \bar{Y}_A)^2 + (Z - \bar{Z}_A)^2 \right]^{1/2}$$

In contrast to equations (16), equations (18) show no dependence on the absolute position of the object.

For each reference star on the photographic plate, both the measured image coordinates x_s, y_s and the corresponding direction cosines λ_s, μ_s, ν_s are known. These quantities are determined from the plate measurements and the right ascension and declination of each reference star as determined from the star catalogs and charts. From a knowledge of the station location and the time of star exposure, the right ascension and declination of each reference star is transformed into the direction cosine relative to the fixed-axis system $\bar{X}, \bar{Y}, \bar{Z}$. Hence, for n reference stars chosen on the photographic plate, $2n$ equations in six unknowns $x_p, y_p, c, \sigma_1, \sigma_2, \sigma_3$ exist for each camera. Approximately 15 reference stars which are well distributed over each photographic plate are used to determine the elements of camera orientation for each camera. The method of solution is identical to that previously described for the position coordinates. The initial approximations to the azimuth, elevation, and roll of the camera $\sigma_1, \sigma_2, \sigma_3$ are obtained from the camera dial readings, and the focal length c is approximated with that supplied by the camera manufacturer. The plate center coordinates x_p, y_p are approximated by their values as computed from measurements of the fiducial marks on the photographic plate. The magnitudes of $\sigma_1, \sigma_2, \sigma_3, x_p, y_p,$ and c which satisfy equations (18) to some prescribed limit are the most probable values for these camera constants. The functional relationships between $\sigma_1, \sigma_2, \sigma_3$ and $\lambda_1, \lambda_2, \dots, \lambda_3$ are derived in reference 6.

VELOCITY AND DECELERATION

The spatial distance corresponding to the length of each shutter break on the plate is determined by the application of one of the foregoing methods. Elapsed time from the beginning to the end of a particular shutter break is determined when the period of revolution of the shutter and shutter configuration are known. After the distances along the reentry trajectory have been properly weighted (in a manner discussed in ref. 3) to account for image quality and readability on the plate, they are fitted by the least-squares method to the following equation which is found in reference 3:

$$d = a_1 + b_1 t + c_1 e^{k_1 t} \quad (19)$$

In equation (19), d and t denote the spatial distance along the reentry trajectory and the time, respectively. The constants a_1, b_1, c_1, k_1 are determined from the least-squares process.

Once the constants are determined, the velocity and deceleration equations result immediately by differentiation; thus

$$\left. \begin{aligned} V &= b_1 + c_1 k_1 e^{k_1 t} \\ \dot{V} &= c_1 k_1^2 e^{k_1 t} \end{aligned} \right\} \quad (20)$$

Hence, the velocity and deceleration at any time along the reentry trajectory are computed by evaluating equations (20) at the desired time.

As described in reference 3, equation (19) is an empirical approximation to the true variation of distance with time along the reentry trajectory. For long reentry images, a better representation of distance as a function of time is obtained when the image is segmented and equation (19) is applied to each segment.

CONCLUDING REMARKS

The three data reduction methods discussed in this report were assembled for application to Langley reentry experiments in which photographic coverage was employed for position and velocity determination. The data reduction method using straight-line approximations to the reentry images (data reduction method I) has been applied extensively to the Trailblazer I and II series of reentry experiments discussed in NASA Technical Notes D-2189 and D-1866 because most of the reentry images obtained were approximately straight-line segments on the plates and in most of the experiments only nonsynchronous photographs were available. The data reduction method utilizing a third-order polynomial approximation to the reentry images (data reduction method II) has been applied to several pairs of plates from the Trailblazer experiments and the results indicate that this method of reduction should be more suitable than data reduction method I where the reentry image shows a definite curvature on the film. However, limited data requiring data reduction method II have been available and a full evaluation of this technique has not been possible. Although the data reduction method using synchronous photographs (data reduction method III) has been checked out with hypothetical data and data from other projects, suitable data from the Trailblazer reentry experiments have not been available for the application of this technique.

Langley Research Center,
 National Aeronautics and Space Administration,
 Langley Station, Hampton, Va., March 28, 1967,
 125-23-02-04-23.

APPENDIX A

RELATIVE STATION COORDINATES AT INSTANT OF REENTRY

In figure 8, R_A and R_B denote the radii from the center of the earth of the two camera stations A and B, respectively. The respective geocentric latitudes are represented by ϕ_A' and ϕ_B' . At the instant of reentry, let θ_A be the sidereal time at station A. The X-axis points toward the mean equinox of date and the Y-axis lies 90° east in the plane of the equator. The Z-axis is chosen to form a right-hand orthogonal system.

From figure 8,

$$X_A = R_A \cos \phi_A' \cos \theta_A$$

$$Y_A = R_A \cos \phi_A' \sin \theta_A$$

$$Z_A = R_A \sin \phi_A'$$

and

$$X_B = R_B \cos \phi_B' \cos(\theta_A + \gamma)$$

$$Y_B = R_B \cos \phi_B' \sin(\theta_A + \gamma)$$

$$Z_B = R_B \sin \phi_B'$$

where γ is the difference in the west longitudes of each site or

$$\gamma = \Lambda_B - \Lambda_A$$

Therefore, the coordinates of camera B with respect to camera A (eqs. (8)) are

$$X_{AB} = X_B - X_A$$

$$Y_{AB} = Y_B - Y_A$$

$$Z_{AB} = Z_B - Z_A$$

APPENDIX A

or

$$X_{AB} = (R_B \cos \phi_B' \cos \gamma - R_A \cos \phi_A') \cos \theta_A - (R_B \cos \phi_B' \sin \gamma) \sin \theta_A$$

$$Y_{AB} = (R_B \cos \phi_B' \sin \gamma) \cos \theta_A + (R_B \cos \phi_B' \cos \gamma - R_A \cos \phi_A') \sin \theta_A$$

$$Z_{AB} = R_B \sin \phi_B' - R_A \sin \phi_A'$$

and the distance between the camera sites is given by

$$R_{AB} = (X_{AB}^2 + Y_{AB}^2 + Z_{AB}^2)^{1/2}$$

APPENDIX B

STANDARD PLATE COORDINATES

The plane tangent to the celestial sphere at the point where the optical axis of the camera intersects the sphere is represented by the hatched area in figure 9. The photographic plate is parallel to this tangent plane. (See ref. 8.) In figure 9, let C denote the center of the unit sphere, C' the point where the optical axis (central ray) intersects the sphere, O an object in the vicinity of C' , O' the projection of the object on the tangent plane, and N the north celestial pole. The components of $C'O'$ along the ξ - and η -axes are defined to be the standard coordinates of that particular object. The η -axis increases in a northerly direction corresponding to increasing declination. The ξ -axis is the projection of the parallel of declination through the tangent point and increases in an easterly direction corresponding to increasing right ascension. The origin of the standard coordinate system is the point of tangency, and the η -axis is the projection of a meridian through the tangent point onto the projection plane.

From figure 9,

$$\tan \psi = \frac{C'O'}{CC'} = C'O' \quad (21)$$

where ψ is the angle between the optical axis and the object ray. Also, from the figure,

$$\left. \begin{aligned} \xi_0 &= C'O' \sin \theta = \sin \theta \tan \psi \\ \eta_0 &= C'O' \cos \theta = \cos \theta \tan \psi \end{aligned} \right\} \quad (22)$$

If the direction cosines in an astronomical equatorial coordinate system of the object ray CO and the optical axis CC' are denoted by λ_0, μ_0, ν_0 and λ_c, μ_c, ν_c , respectively, then

$$\cos \psi = \lambda_0 \lambda_c + \mu_0 \mu_c + \nu_0 \nu_c \quad (23)$$

where

$$\begin{aligned} \lambda_0 &= \cos \delta_0 \cos \alpha_0 & \lambda_c &= \cos \delta_c \cos \alpha_c \\ \mu_0 &= \cos \delta_0 \sin \alpha_0 & \mu_c &= \cos \delta_c \sin \alpha_c \\ \nu_0 &= \sin \delta_0 & \nu_c &= \sin \delta_c \end{aligned}$$

APPENDIX B

and α_o, δ_o and α_c, δ_c represent the right ascension and declination of the object ray and optical axis, respectively.

By use of equation (23), equations (22) become

$$\left. \begin{aligned} \xi_o &= \frac{\sin \theta \sin \psi}{\lambda_o \lambda_c + \mu_o \mu_c + \nu_o \nu_c} \\ \eta_o &= \frac{\cos \theta \sin \psi}{\lambda_o \lambda_c + \mu_o \mu_c + \nu_o \nu_c} \end{aligned} \right\} \quad (24)$$

From the spherical triangle OC'N in figure 9,

$$\left. \begin{aligned} \sin \psi \cos \theta &= \sin \delta_o \cos \delta_c - \cos \delta_o \sin \delta_c \cos(\alpha_o - \alpha_c) \\ \sin \psi \sin \theta &= \cos \delta_o \sin(\alpha_o - \alpha_c) \end{aligned} \right\} \quad (25)$$

From figure 10, the direction cosines of the ξ -axis are

$$\left. \begin{aligned} \lambda_\xi &= \cos 0 \cos\left(\alpha_c + \frac{\pi}{2}\right) = -\sin \alpha_c \\ \mu_\xi &= \cos 0 \sin\left(\alpha_c + \frac{\pi}{2}\right) = \cos \alpha_c \\ \nu_\xi &= \sin 0 = 0 \end{aligned} \right\} \quad (26)$$

and those of the η -axis are

$$\left. \begin{aligned} \lambda_\eta &= \cos\left(\delta_c + \frac{\pi}{2}\right) \cos \alpha_c = -\sin \delta_c \cos \alpha_c \\ \mu_\eta &= \cos\left(\delta_c + \frac{\pi}{2}\right) \sin \alpha_c = -\sin \delta_c \sin \alpha_c \\ \nu_\eta &= \sin\left(\delta_c + \frac{\pi}{2}\right) = \cos \delta_c \end{aligned} \right\} \quad (27)$$

Substituting equations (26) and (27) along with expressions for λ_o, μ_o, ν_o into equations (25) yields

APPENDIX B

$$\left. \begin{aligned} \sin \psi \cos \theta &= \lambda_0 \lambda_\eta + \mu_0 \mu_\eta + \nu_0 \nu_\eta \\ \sin \psi \sin \theta &= \lambda_\xi \lambda_0 + \mu_\xi \mu_0 \end{aligned} \right\} \quad (28)$$

Hence, substitution of equations (28) into equations (24) gives

$$\xi_0 = \frac{\lambda_0 \lambda_\xi + \mu_0 \mu_\xi}{\lambda_0 \lambda_c + \mu_0 \mu_c + \nu_0 \nu_c}$$

$$\eta_0 = \frac{\lambda_0 \lambda_\eta + \mu_0 \mu_\eta + \nu_0 \nu_\eta}{\lambda_0 \lambda_c + \mu_0 \mu_c + \nu_0 \nu_c}$$

APPENDIX C

POSITION OF CURVED REENTRIES

In figure 6, λ_i, μ_i, ν_i define line U constrained to pass through the center of projection of camera A and some point on the curved reentry. These direction cosines are obtained by evaluating the polynomial fit through the reentry image at some point x_i, y_i and using equations (10) and (12). The equation of the line U relative to the astronomical equatorial system X, Y, Z can be written as

$$\frac{X}{\lambda_i} = \frac{Y}{\mu_i} = \frac{Z}{\nu_i} \quad (29)$$

Let u be some general point on line U. The coordinates of u are $X_u, \left(\frac{\mu_i}{\lambda_i}\right)X_u, \left(\frac{\nu_i}{\lambda_i}\right)X_u$. Line Q constrained to pass through the center of projection of camera B (chopping camera) and some point on the reentry corresponding to some shutter break on photographic plate B is defined by direction cosines λ_j, μ_j, ν_j . The equation of line Q becomes

$$\frac{X - X_{AB}}{\lambda_j} = \frac{Y - Y_{AB}}{\mu_j} = \frac{Z - Z_{AB}}{\nu_j}$$

Some general point q on line Q has coordinates $X_q, (X_q - X_{AB})\frac{\mu_j}{\lambda_j} + Y_{AB}, (X_q - X_{AB})\frac{\nu_j}{\lambda_j} + Z_{AB}$. The distance between the two points u and q is given by

$$D = \left\{ (X_u - X_q)^2 + \left[\frac{\mu_i}{\lambda_i} X_u - \frac{\mu_j}{\lambda_j} (X_q - X_{AB}) - Y_{AB} \right]^2 + \left[\frac{\nu_i}{\lambda_i} X_u - \frac{\nu_j}{\lambda_j} (X_q - X_{AB}) - Z_{AB} \right]^2 \right\}^{1/2}$$

Expressions for X_u and X_q , in terms of the direction cosines of the two lines, which give a minimum value of D, are determined from

$$\frac{\partial D}{\partial X_u} = 0$$

and

$$\frac{\partial D}{\partial X_q} = 0$$

APPENDIX C

Solving the two resulting equations for X_u and X_q yields

$$\left. \begin{aligned} X_u &= \frac{\lambda_i(B_i - C_j A_{ij})}{1 - A_{ij}^2} \\ X_q &= \frac{\lambda_j(B_i A_{ij} - C_j)}{1 - A_{ij}^2} + X_{AB} \end{aligned} \right\} \quad (30)$$

where

$$B_i = \lambda_i X_{AB} + \mu_i Y_{AB} + \nu_i Z_{AB}$$

$$C_j = \lambda_j X_{AB} + \mu_j Y_{AB} + \nu_j Z_{AB}$$

and

$$A_{ij} = \lambda_i \lambda_j + \mu_i \mu_j + \nu_i \nu_j$$

Substitution of X_u and X_q as given by equations (30) into the equation for D gives rise to an expression for the minimum distance between the two lines defined by direction cosines λ_i, μ_i, ν_i and λ_j, μ_j, ν_j . The resulting expression for D is a function of the direction cosines and the relative location of the two cameras.

The set of direction cosines λ_i, μ_i, ν_i which gives D a minimum value is found by using the numerical scheme discussed in the text. The X, Y, Z coordinates of the j th shutter break, relative to camera A , are then determined from equations (29) and (30). Hence,

$$X_{Aj} = \frac{\lambda_i(B_i - C_j A_{ij})}{1 - A_{ij}^2}$$

$$Y_{Aj} = \frac{\mu_i}{\lambda_i} X_{Aj}$$

$$Z_{Aj} = \frac{\nu_i}{\lambda_i} X_{Aj}$$

and the slant range from station A to the intersection point is

$$R_{Aj} = \left(X_{Aj}^2 + Y_{Aj}^2 + Z_{Aj}^2 \right)^{1/2} = \frac{B_i - C_j A_{ij}}{1 - A_{ij}^2}$$

REFERENCES

1. Gardner, William N.; Brown, Clarence A., Jr.; Henning, Allen B.; Hook, W. Ray; Lundstrom, Reginald R.; and Ramsey, Ira W., Jr.: Description of Vehicle System and Flight Tests of Nine Trailblazer I Reentry Physics Research Vehicles. NASA TN D-2189, 1964.
2. Lundstrom, Reginald R.; Henning, Allen B.; and Hook, W. Ray: Description and Performance of Three Trailblazer II Reentry Research Vehicles. NASA TN D-1866, 1964.
3. Whipple, Fred L.; and Jacchia, Luigi G.: Reduction Methods for Photographic Meteor Trails. Smithsonian Contrib. Astrophys., vol. 1, no. 2, 1957, pp. 183-206.
4. H.M. Nautical Almanac Office: Planetary Co-Ordinates for the Years 1960-1980 Referred to the Equinox of 1950.0. Her Majesty's Stationery Office, 1958.
5. Anon.: The American Ephemeris and Nautical Almanac for the Year 1965. U.S. Naval Obs., 1963.
6. Brown, Duane C.: A Treatment of Analytical Photogrammetry. AFMTC-TR-57-22, ASTIA Doc. No. 124144, U.S. Air Force, Aug. 20, 1957.
7. Nielsen, Kaj L.: Methods in Numerical Analysis. The Macmillan Co., c.1956.
8. Smart, W. M.: Text-Book on Spherical Astronomy. Fourth ed., Cambridge Univ. Press, 1944. (Reprinted 1956.)

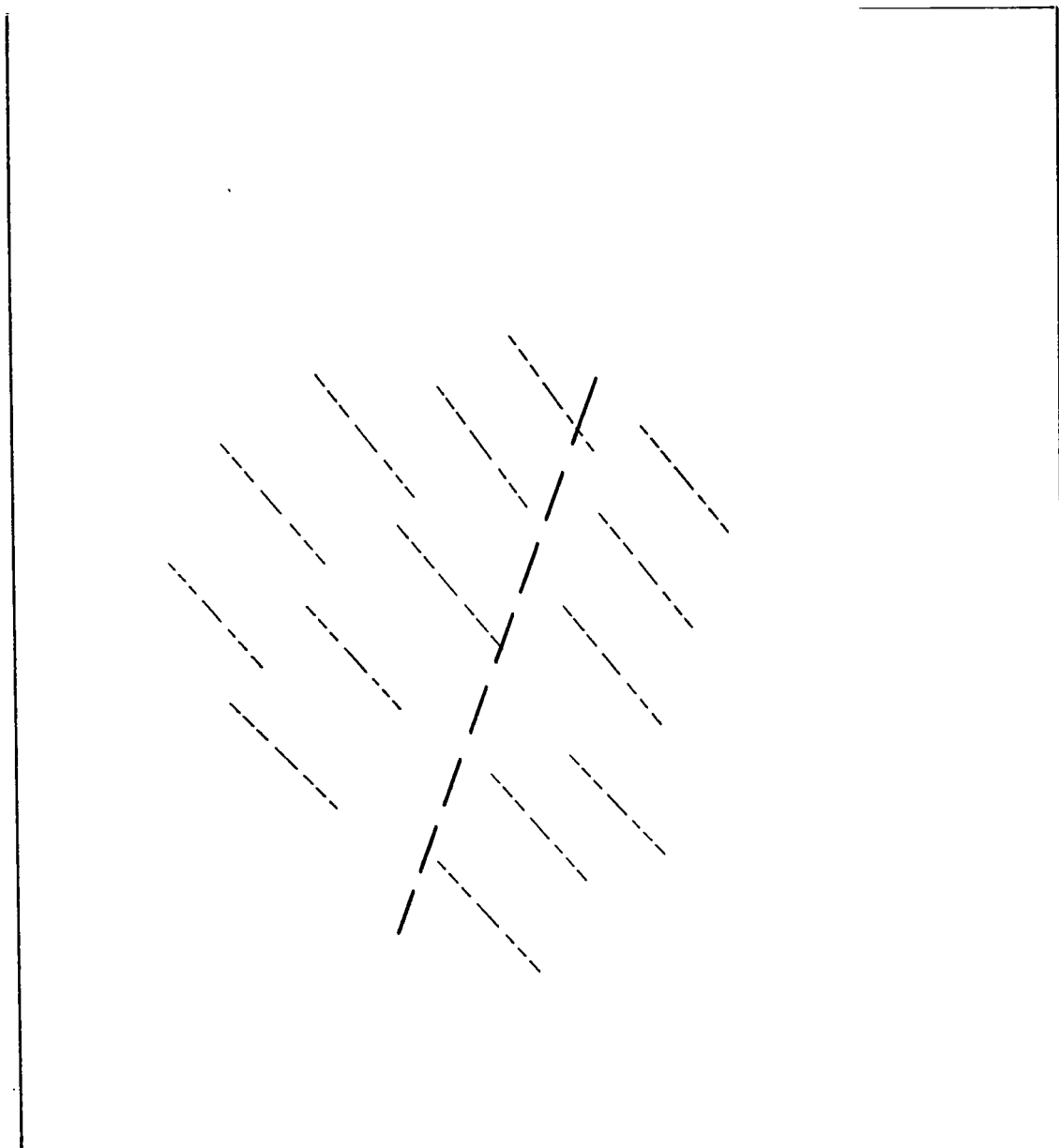


Figure 1.- Sketch of chopped photograph of a reentry against a star background.

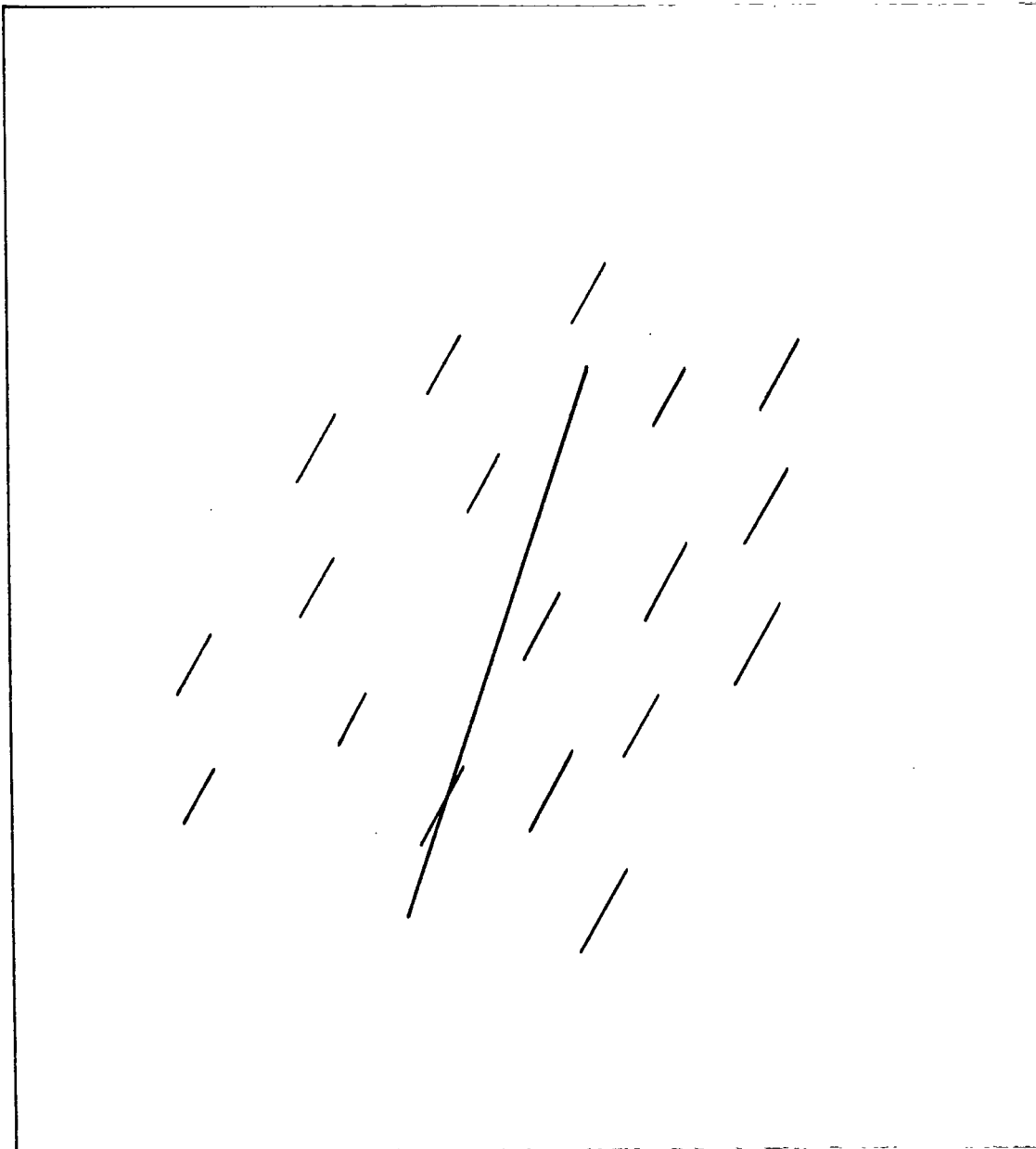


Figure 2.- Sketch of streaked photograph of a reentry against a star background.

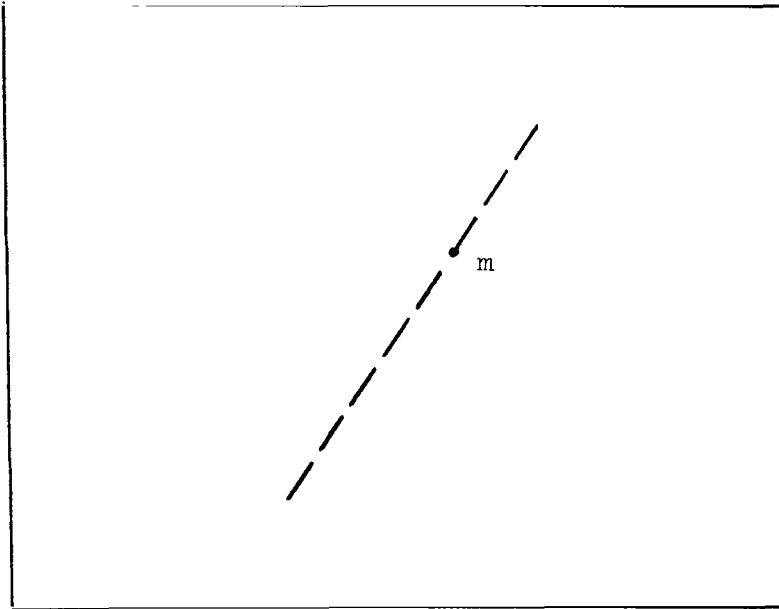


Plate A

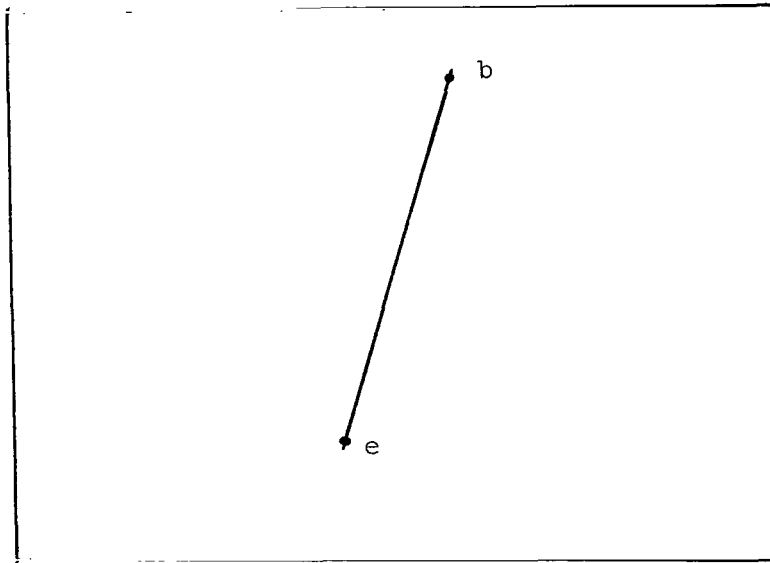


Plate B

Figure 3.- Photographic plate schematics of reentry points used in the data reduction methods.

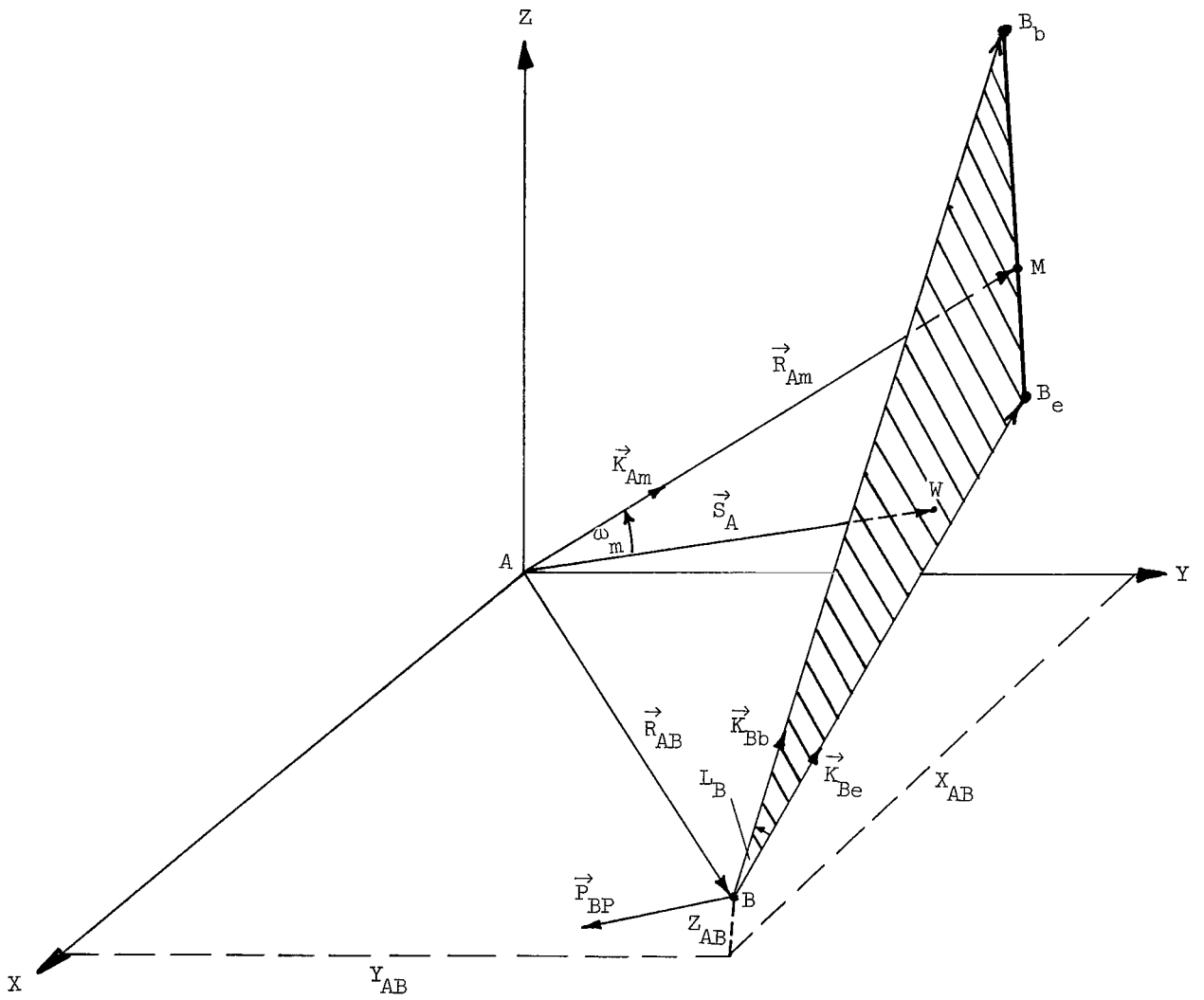


Figure 4.- Relationship between the reentry and the cameras.

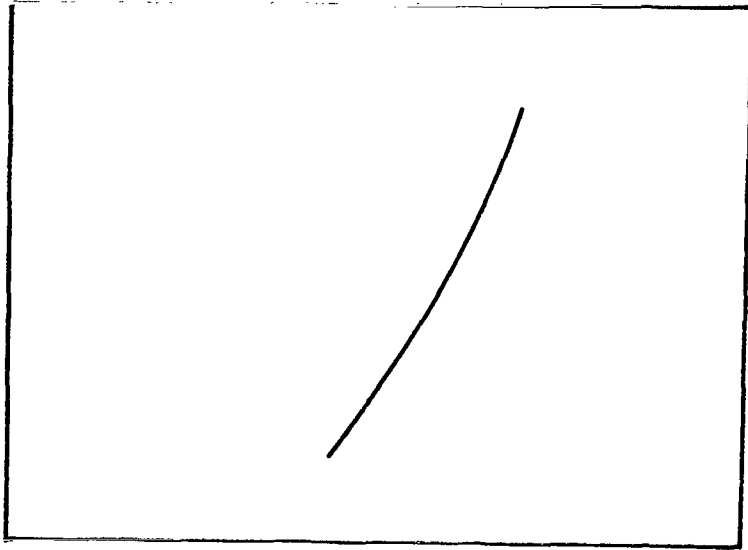


Plate A

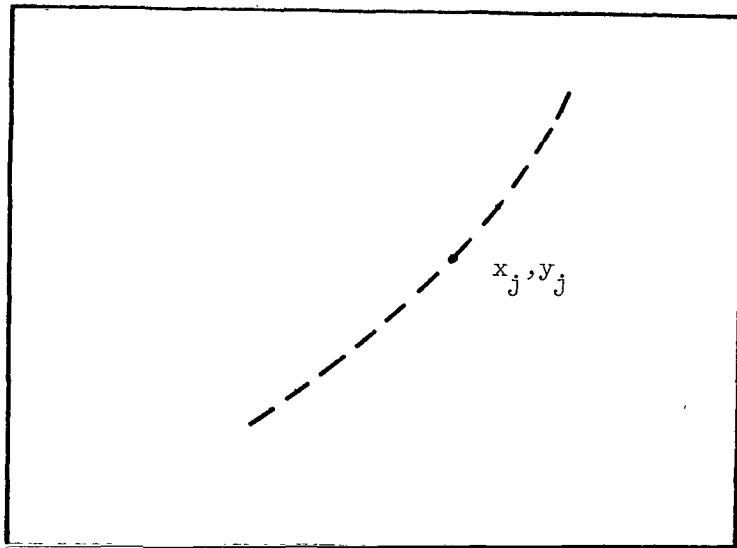


Plate B

Figure 5.- Illustration of curved reentry photographs.

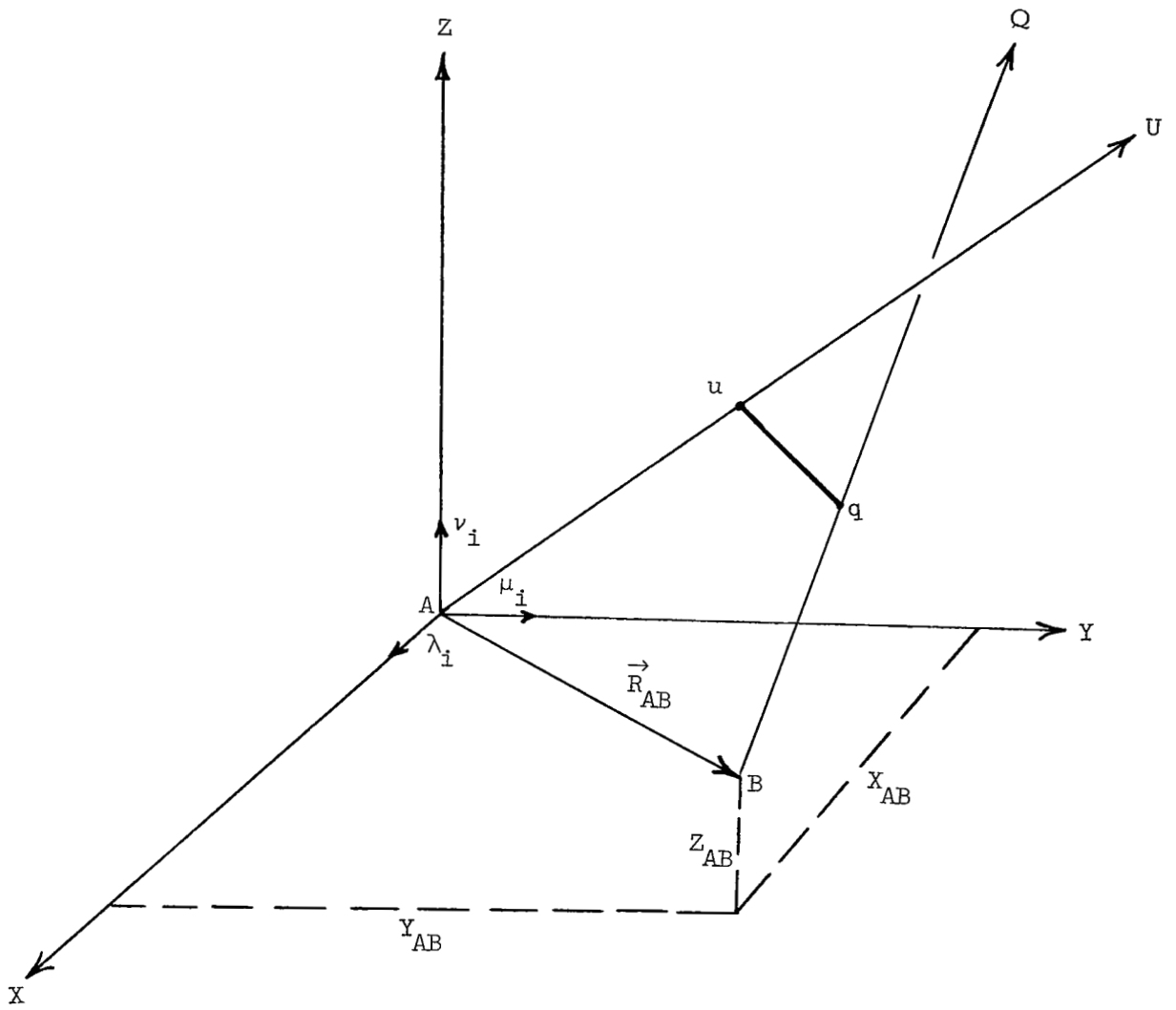


Figure 6.- Geometry employed in the curved reentry method.

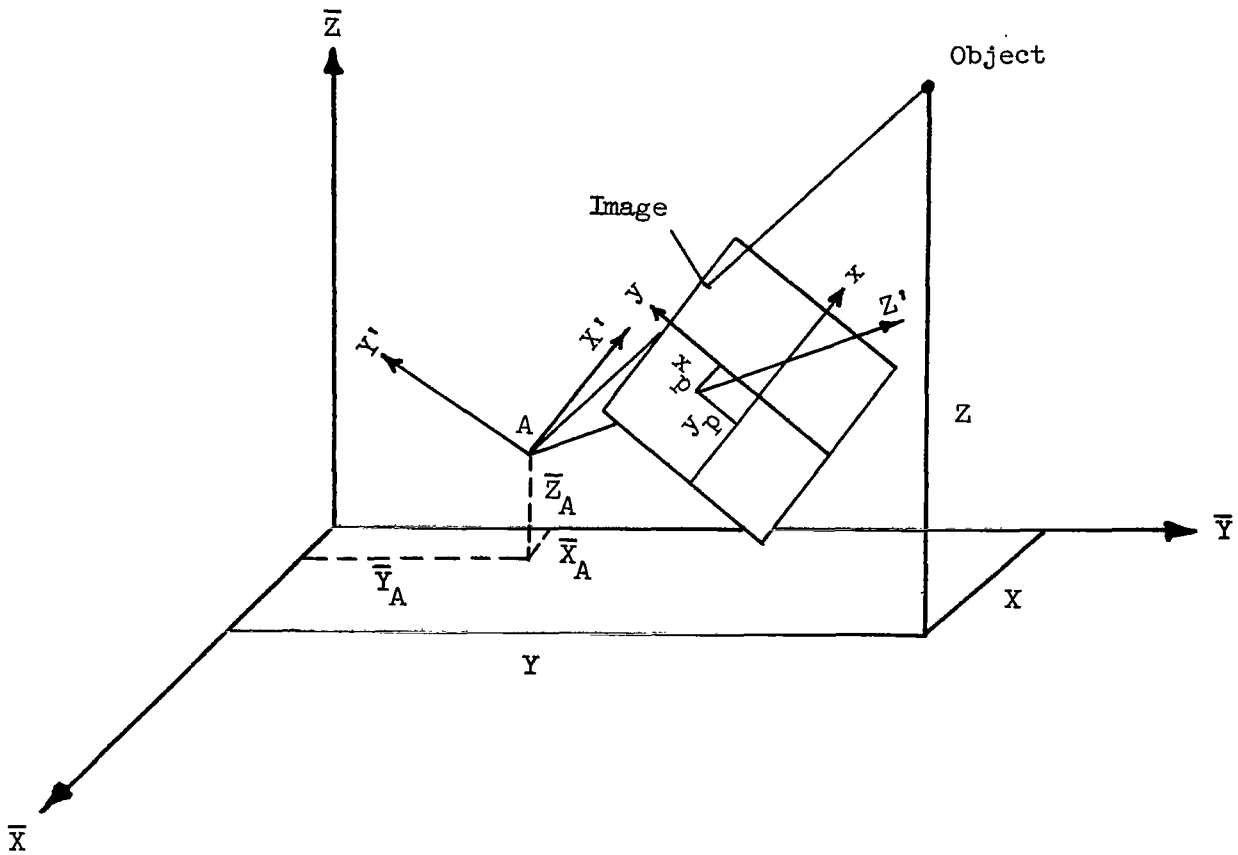


Figure 7.- Axis systems associated with the point-by-point triangulation method.

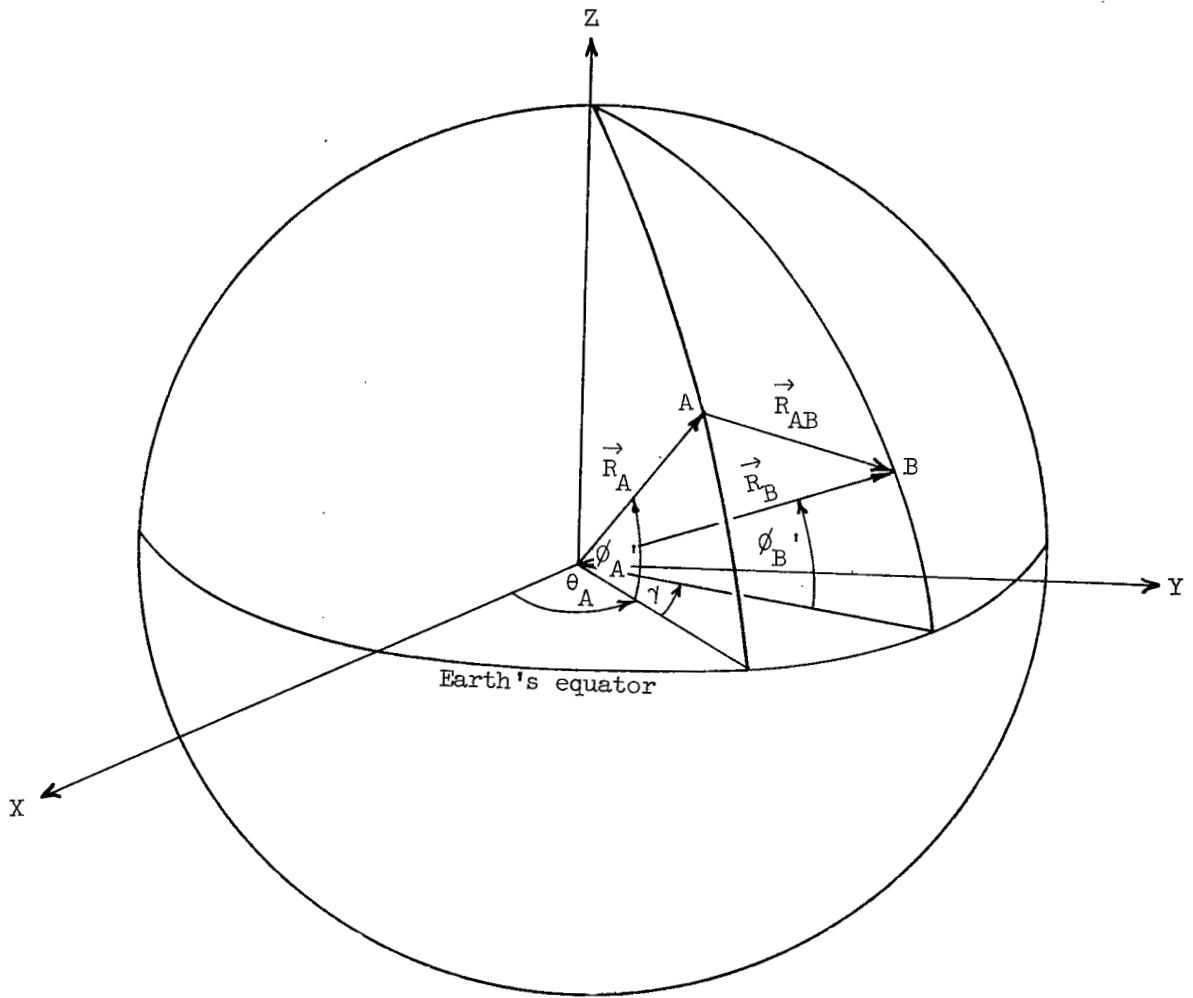


Figure 8.- Relative station coordinates at instant of reentry.

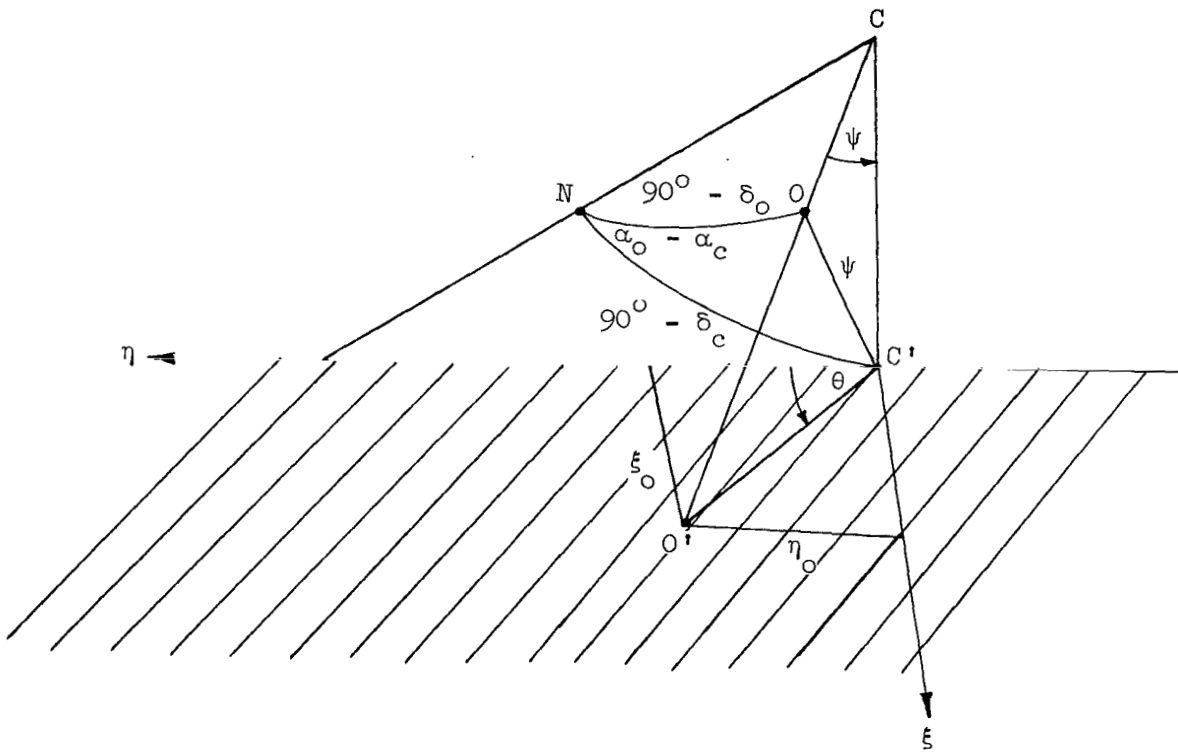


Figure 9.- Standard plate coordinates.

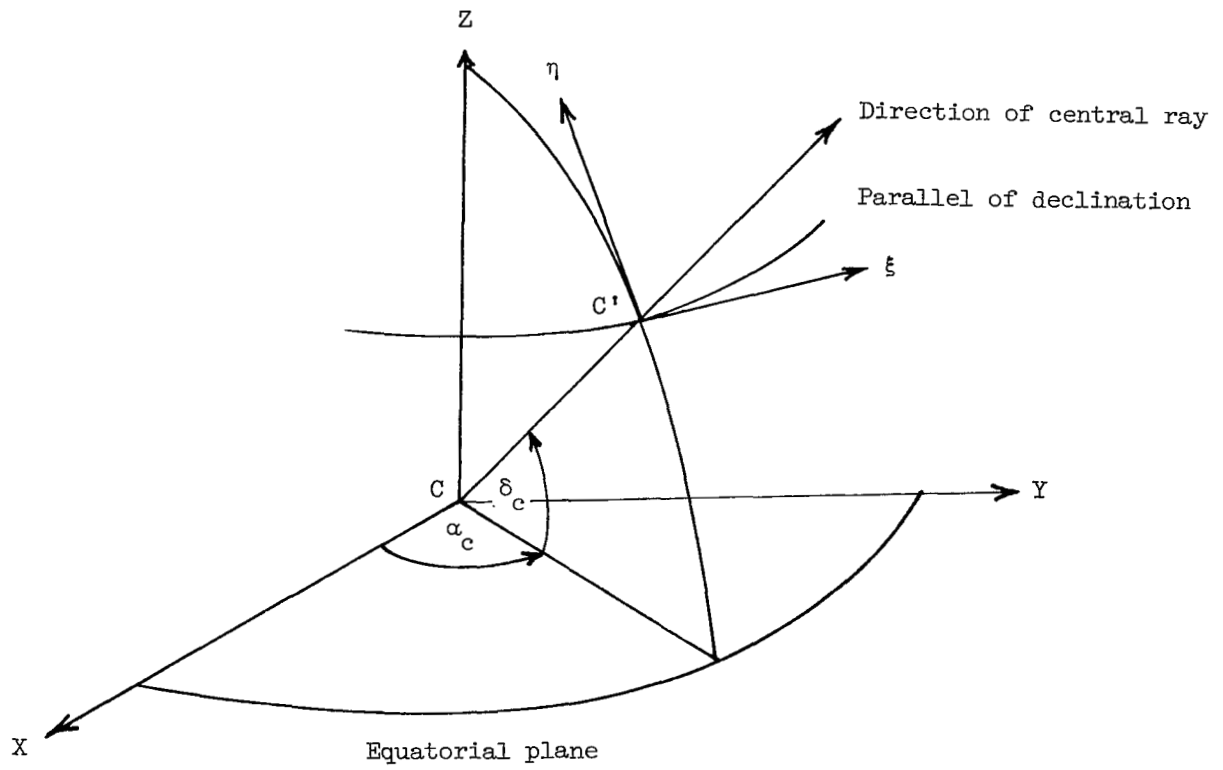


Figure 10.- Standard plate coordinate axes.

"The aeronautical and space activities of the United States shall be conducted so as to contribute . . . to the expansion of human knowledge of phenomena in the atmosphere and space. The Administration shall provide for the widest practicable and appropriate dissemination of information concerning its activities and the results thereof."

—NATIONAL AERONAUTICS AND SPACE ACT OF 1958

NASA SCIENTIFIC AND TECHNICAL PUBLICATIONS

TECHNICAL REPORTS: Scientific and technical information considered important, complete, and a lasting contribution to existing knowledge.

TECHNICAL NOTES: Information less broad in scope but nevertheless of importance as a contribution to existing knowledge.

TECHNICAL MEMORANDUMS: Information receiving limited distribution because of preliminary data, security classification, or other reasons.

CONTRACTOR REPORTS: Scientific and technical information generated under a NASA contract or grant and considered an important contribution to existing knowledge.

TECHNICAL TRANSLATIONS: Information published in a foreign language considered to merit NASA distribution in English.

SPECIAL PUBLICATIONS: Information derived from or of value to NASA activities. Publications include conference proceedings, monographs, data compilations, handbooks, sourcebooks, and special bibliographies.

TECHNOLOGY UTILIZATION PUBLICATIONS: Information on technology used by NASA that may be of particular interest in commercial and other non-aerospace applications. Publications include Tech Briefs, Technology Utilization Reports and Notes, and Technology Surveys.

Details on the availability of these publications may be obtained from:

SCIENTIFIC AND TECHNICAL INFORMATION DIVISION
NATIONAL AERONAUTICS AND SPACE ADMINISTRATION

Washington, D.C. 20546